Active Thermal Control for Power Semiconductor using Peltier-Device

Masamichi Yamaguchi
Department of Science of Technology Innovation
Nagaoka University of Technology
Nagaoka, Japan
m_yamaguchi@stn.nagaokaut.ac.jp

Hiroki Watanabe
Department of Electrical, Electronics and Information Engineering
Nagaoka University of Technology
Nagaoka, Japan
hwatanabe@vos.nagaokaut.ac.jp

Jun-ichi Itoh
Department of Science of Technology Innovation
Nagaoka University of Technology
Nagaoka, Japan
itoh@vos.nagaokaut.ac.jp

Kyo-Beum Lee
Department of Electrical and Computer Engineering
Ajou University
Suwon, South Korea
kyl@ajou.ac.kr

***Abstract*— The paper proposes an Active Thermal Control (ATC) approach employing a Peltier device as a heat exchanger for temperature regulation. The control strategy relies on Model Predictive Control (MPC) utilizing an equivalent thermal model. It elucidates the current control methodology for the Peltier device based on this model and predicted temperature. Moreover, the predicted temperature and additional thermal sensor estimate the loss amount at the heat source without any electrical sensor, such as a current or a voltage sensor. The simulation result affirms the effectiveness of the proposed control and loss estimation method. Finally, the experimental result demonstrates the validity of the proposed control, evidenced by a 2.6% maximum error in temperature control.**

Keywords*— *Active Thermal Control (ATC), Model Predictive Control (MPC), Peltier-device

I. INTRODUCTION

The growing demand for power conversion circuits, driven by the proliferation of distributed power supply systems and Electric Vehicles (EVs), underscores the need for robust solutions. To address the challenges posed by high-temperature environments, power semiconductor technology has evolved to enable operation within these conditions, particularly in applications like EVs [1]. However, despite advancements in high-temperature-capable devices, ensuring the reliability of power converters remains paramount. Power device failures, often stemming from issues such as the lift-off of bonding wires and solder cracks, are closely linked to thermal cycling. Even with the integration of high-temperature devices, these failure mechanisms persist. Consequently, reliability concerns related to thermal cycling continue to plague power converters. Effectively mitigating the impact of thermal cycling on power device reliability presents a significant challenge for the industry. Strategies aimed at enhancing the durability and longevity of power converters in high-temperature environments are crucial for meeting the evolving demands of modern power systems [2].

Active Thermal Control (ATC) has emerged as a key area of research aimed at mitigating thermal cycling in power semiconductors [3-5]. The primary objective of ATC is to reduce power loss, as this directly impacts thermal cycling. Strategies such as managing switching frequency or pattern alteration are commonly employed to achieve loss reduction. However, adjustments to these parameters can affect circuit operation and performance metrics like Total Harmonic Distortion (THD). To address this, weighting functions are often used to determine optimal switching frequency or pattern, although maximizing loss reduction remains challenging even with their application. An alternative approach to ATC involves thermal structure optimization to minimize the influence on circuit operation [6-8]. For instance, reference [8] utilized a Peltier device as a heat exchanger. While experimental results demonstrated significant reductions in device temperature, thermal cycling persisted due to the absence of temperature-based Peltier device control. Efforts to refine ATC methodologies are ongoing, with researchers exploring novel techniques to enhance thermal management while minimizing disruption to circuit operation. Achieving comprehensive thermal control without compromising circuit performance remains a complex yet crucial objective in the development of reliable power converters.

This paper introduces an Active Thermal Control (ATC) method for power devices utilizing a Peltier device in conjunction with Model Predictive Control (MPC). The proposed approach leverages the thermal model of the Peltier device to implement MPC, whereby the predicted temperature guides the generation of current commands for the Peltier device to regulate temperature. Both simulation and experimental results validate the efficacy of this thermal control strategy employing the Peltier device.

II. Thermal Structure of Proposed ATC

A. Heat dissipation structure

Fig. 1 shows the thermal structure of the proposed method. A Peltier device is positioned between the power device and the heatsink, facilitating thermal regulation. Additionally, a heat spreader is integrated to enhance the conduction of heat flow. Notably, the Peltier device and the power device are not isolated, as the cold side thermal resistance directly influences thermal control. Consequently, the endotherm value of the Peltier device plays a crucial role in controlling the temperature of the device.

B. Peltier device

Fig. 2 depicts the thermal equivalent circuit of the Peltier device. Within this circuit, T_c and T_h represent the temperatures of the cold side and heated side, respectively. R_{th_p} denotes the thermal resistance, while C_{th} represents the capacitance. Q_{cold} signifies the endotherm on the cold side, whereas Q_{hot} represents the heat generation on the heated side. This circuit provides a simplified representation of the thermal dynamics of the Peltier device, facilitating analysis and control.

Exactly, the current flowing through the Peltier device and the temperatures on each side directly influence the heat transfer across the device. Therefore, to control the endotherm value (Q_{cold}) on the cold side and the heat generation (Q_{hot}) on the heated side, precise management of the current command is essential. By adjusting the current command appropriately, it's possible to regulate the thermal behavior of the Peltier device

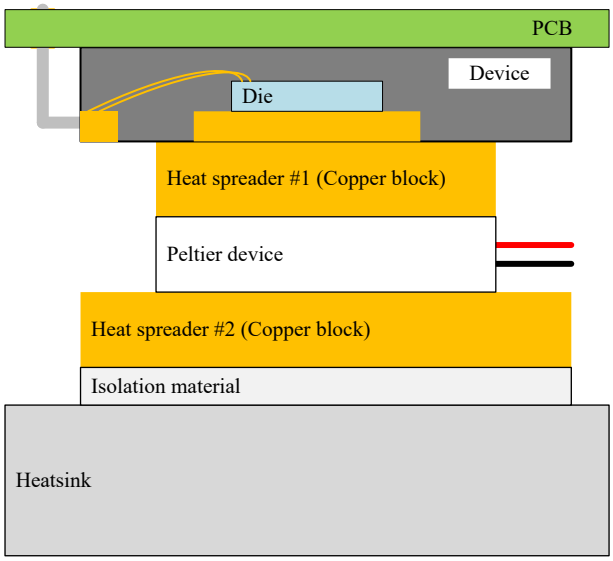

Fig. 1. Thermal structure of proposed ATC.

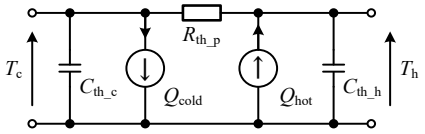

Fig. 2. Thermal model of Peltier-device.

and consequently control temperatures within the system. Then, the endotherm is expressed by

$$Q_{cold} = S_p T_c I_p - \frac{1}{2} r_p I_p^{\,2} - \frac{T_h - T_c}{R_{th\_p}}, \tag{1}$$

where S_p is the Seebeck coefficient, r_p is electric resistance, and I_p is the current of the Peltier device. The first term expresses the endotherm by the Peltier effect. The Second term expresses the Joule heat on the cold side. The heat generation on the heated-side Q_{hot} is also expressed by

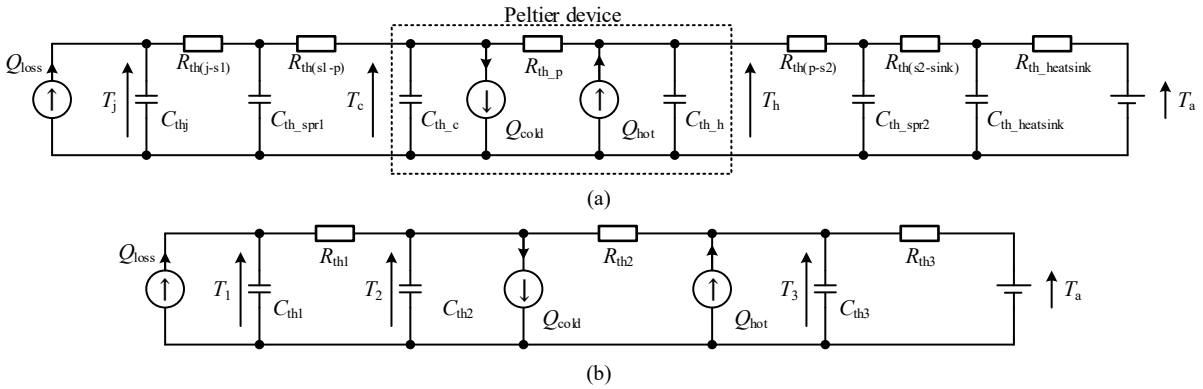

Fig. 3. Thermal model based on heat dissipation structure (a) Full model (b) Simplified model.

$$Q_{\text{hot}} = S_p T_h I_p + \frac{1}{2} r_p {I_p}^2 - \frac{T_\text{h} - T_\text{c}}{R_{\text{th\_p}}} . \quad (2)$$

Fig. 3a presents the comprehensive equivalent thermal model, incorporating the detailed representation of the Peltier device and thermal resistances. In contrast, Fig. 3b offers a simplified version of Fig. 3a. Notably, Fig. 3b disregards the thermal resistance between spreader #1 and the Peltier device, as well as between the Peltier device and the heatsink, to streamline the model. Then, the thermal capacitance C_{th1} is the sum of the $C_{\text{th,spr1}}$ and the $C_{\text{th,c}}$, and the C_{th3} is the sum of the $C_{\text{th,h}}$ and the $C_{\text{th,spr2}}$.

III. Thermal Control Based on Model Predictive Control

A. Thermal model for temperature prediction

The current command of the Peltier device is derived from the predictive temperature based on the thermal model. The predicted temperature is expressed by

$$T_1^{\text{P}}(k+1) = \frac{1}{C_{\text{th1}}} \left\{ Q_{\text{loss}}(k) - \frac{T_1(k) - T_2(k)}{R_{\text{th1}}} \right\} \Delta t + T_1(k) , \quad (3)$$

$$T_2^{\text{P}}(k+1) = \frac{1}{C_{\text{th2}}} \left\{ -Q_{\text{cold}}(k) + \frac{T_1(k) - T_2(k)}{R_{\text{th1}}} - \frac{T_2(k) - T_3(k)}{R_{\text{th2}}} \right\} \Delta t + T_2(k) , \quad (4)$$

$$T_3^{\text{P}}(k+1) = \frac{1}{C_{\text{th3}}} \left\{ Q_{\text{hot}}(k) + \frac{T_2(k) - T_3(k)}{R_2} - \frac{T_3(k) - T_\text{a}(k)}{R_{\text{th3}}} \right\} \Delta t + T_3(k) , \quad (5)$$

where Δt is the time step of the controller, k expresses the current instance, and k+1 expresses the next instance. Then, the predicted temperature $T_1^{\text{P}}(k+3)$ is also expressed by

$$T_1^{\text{P}}(k+3) = \frac{1}{C_{\text{th1}}} \left\{ Q_{\text{loss}}(k+2) - \frac{T_1^{\text{P}}(k+2) - T_2^{\text{P}}(k+2)}{R_{\text{th1}}} \right\} \Delta t + T_1^{\text{P}}(k+2) . \quad (6)$$

B. Temperature control with Peltier device

The temperature command of the $T_2^*(k+2)$ is derived using (6) by

$$T_2^*(k+2) = \left\{ T_1^*(k+3) - T_1^{\text{P}}(k+2) \right\} \frac{R_{\text{th1}} C_{\text{th1}}}{\Delta t} + T_1^{\text{P}}(k+2) - R_{\text{th1}} Q_{\text{loss}}(k) , \quad (7)$$

where $T_1^*(k+3)$ is the target temperature of T_1, and $T_2^*(k+2)$ is the command temperature of T_2. The endotherm command $Q_{\text{cold}}^*(k+1)$ is derived using (4) and (7) by

$$Q_{\text{cold}}^*(k+1) = \frac{T_1^{\text{P}}(k+1) - T_2^{\text{P}}(k+1)}{R_{\text{th1}}} - \frac{T_2^{\text{P}}(k+1) - T_3^{\text{P}}(k+1)}{R_{\text{th2}}} - \left\{ T_2^*(k+2) - T_2^{\text{P}}(k+1) \right\} \frac{C_{\text{th2}}}{\Delta t} . \quad (8)$$

The current of the Peltier device determines the endotherm value on the cold side. The current command is derived using (1) and the endotherm command $Q_{\text{cold}}^*(k+1)$ by

$$I_\text{p}^*(k+1) = \frac{S_\text{p} T_2^{\text{P}}(k+1)}{r_\text{p}} - \sqrt{\left(\frac{S_\text{p} T_2^{\text{P}}(k+1)}{r_\text{p}} \right)^2 - \frac{2 Q_{\text{cold}}^*(k+1)}{r_\text{p}}} . \quad (9)$$

C. Loss estimation based on MPC

The proposed ATC requires an accurate loss amount at the heat source to predict the temperature accurately. However, a loss measurement or estimation at the heat source requires additional current sensors and voltage sensors because of the conducting loss and the switching loss should be considered. Such as sensors make a complexity of the circuit implementation. Moreover, the loss estimation makes a huge calculation burden to the controller. Thus, the loss estimation method without a huge calculation burden and additional electrical sensors is required for the proposed ATC.

Then, the thermal sensor is added to measure the actual temperature T_2. The actual loss amount at the heat source Q_{loss} is estimated by the difference between the measured temperature and the predicted one. The predicted temperature at the current instance based on the (4) is expressed by

$$T_2^{\text{P}}(k) = \left\{ -Q_{\text{cold}}(k-1) + \frac{T_1(k-1) - T_2^{\text{R}}(k-1)}{R_{\text{th1}}} - \frac{T_2^{\text{R}}(k-1) - T_3(k-1)}{R_{\text{th2}}} \right\} \frac{\Delta t}{C_{\text{th2}}} + T_2^{\text{R}}(k-1) \quad (10),$$

where T_2^{R} expresses the measured temperature, k-1 expresses the previous instance. Then, the predicted temperature at the current instance $T_2^{\text{P}}(k)$ is predicted at the previous instance.

On the other hand, the actual temperature at the current instance is measured by the thermal sensor. Then, the actual temperature $T_2^{\text{R}}(k)$ is also expressed by

$$T_2^{\text{R}}(k) = \left\{ -Q_{\text{cold}}(k-1) + \frac{T_1^{\text{M}}(k-1) - T_2^{\text{R}}(k-1)}{R_{\text{th1}}} - \frac{T_2^{\text{R}}(k-1) - T_3(k-1)}{R_{\text{th2}}} \right\} \frac{\Delta t}{C_{\text{th2}}} + T_2^{\text{R}}(k-1) \quad (11),$$

where T_1^{M} expresses the modified temperature. The modified temperature should be modified by the difference between the predicted temperature $T_2^{\text{P}}(k)$ and the measured temperature

$T_2^{\mathrm{R}}(k)$. The temperature difference is expressed using (10) and (11) by

$$T_2^{\mathrm{P}}(k) - T_2^{\mathrm{R}}(k) = \frac{1}{R_{\mathrm{th1}} C_{\mathrm{th2}}} \left\{ T_1(k-1) - T_1^{\mathrm{M}}(k-1) \right\} \Delta t \qquad (12).$$

Then, the modified temperature $T_1^{\mathrm{M}}(k\text{-}1)$ is expressed by

$$T_1^{\mathrm{M}}(k-1) = \left\{ T_2^{\mathrm{R}}(k) - T_2^{\mathrm{P}}(k) \right\} \frac{R_{\mathrm{th1}} C_{\mathrm{th2}}}{\Delta t} + T_1(k-1) \qquad (13).$$

The loss amount at the heat source is estimated using modified temperature $T_1^{\mathrm{M}}(k\text{-}1)$. The estimated loss $Q_{\mathrm{loss}}{}^{\mathrm{E}}(k\text{-}2)$ is derived using (3) and (13) by

$$Q_{\mathrm{loss}}{}^{\mathrm{E}}(k-2) = \left\{ T_1^{\mathrm{M}}(k-1) - T_1^{\mathrm{M}}(k-2) \right\} \frac{C_{\mathrm{th1}}}{\Delta t} + \frac{T_1^{\mathrm{M}}(k-2) - T_2^{\mathrm{R}}(k-2)}{R_{\mathrm{th1}}} \qquad (14).$$

Then, the modified temperature $T_1^{\mathrm{M}}(k\text{-}2)$ is the previous instant value of $T_1^{\mathrm{M}}(k\text{-}1)$.

IV. Simulation

The simulation confirms the accuracy of the forecasted temperature and the resultant current command. PLECS serves as the simulation software, and the simulation circuit mirrors Fig. 3b. Table 1 provides an overview of the simulation parameters. Specifically, the loss amount undergoes a step change from 5 W to 20 W, facilitating an evaluation of the step response concerning the predicted temperature. Each temperature is initialized as 26 ℃. Additionally, each predicted temperature is utilized as the previous temperature at the next instance.

A. Temperature prediction and control

As a first step, the predicted temperature and the control are checked in the simulation. The controller uses the loss amount at the current instance as the known parameter to check the temperature prediction itself.

In Fig. 4a, the simulation result utilizing the proposed control is depicted, whereas Fig. 4b illustrates the outcome without employing the control. Despite abrupt changes in loss amounts, the predicted values closely align with the simulated values. Notably, the maximum temperature fluctuation of T_1 remains within a narrow range of 0.2°C, indicating the efficacy of the proposed control method in stabilizing temperatures.

B. Loss estimation based on MPC

As a second step, the loss estimation based on the (14) is checked in the simulation. The estimated loss is utilized in temperature prediction and control. Equation (14) only estimates the loss amount at the two instances ago. Thus, the temperature prediction utilizes the estimated loss at the two instances ago instead of other instance loss. The controller utilizes the actual

TABLE I.

Pertier-device (ETC-288-14-06-E : Adaptive)		
Seebeck coefficient	S_{p}	0.0786 V/K
Electrical resistance	r_{p}	2.7 Ω
Thermal resistance	R_{thp}	0.53 K/W
Thermal equevalent circuit		
Thermal resistance (junction-spreader1)	R_{th1}	0.01 K/W
Thermal resistance of Pertier-device	R_{th2}	0.53 K/W
Thermal resistance (spreader2-air)	R_{th2}	0.18 K/W
Thermal capacitance of heater	C_{th1}	20 J/K
Thermal capacitance (spreader1, cold side)	C_{th2}	316 J/K
Thermal capacitance (hot side, spreader2)	C_{th3}	664 J/K
Temperature prediction		
Caluculate time step	Δt	100 ms
Loss amount	Q_{loss}	5-20 W
Temperature command	$T_1{}^{*}(\mathrm{k+3})$	26 ℃

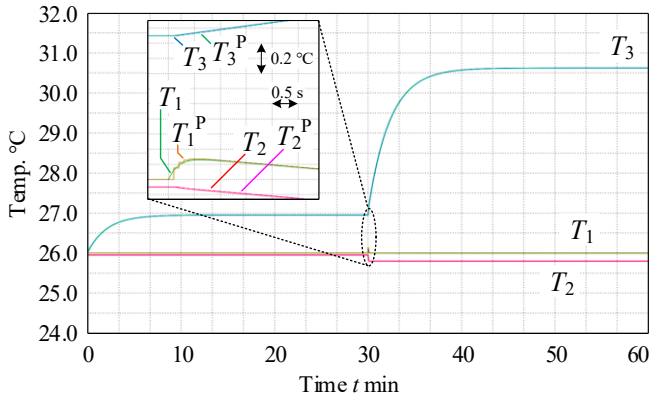

(a)

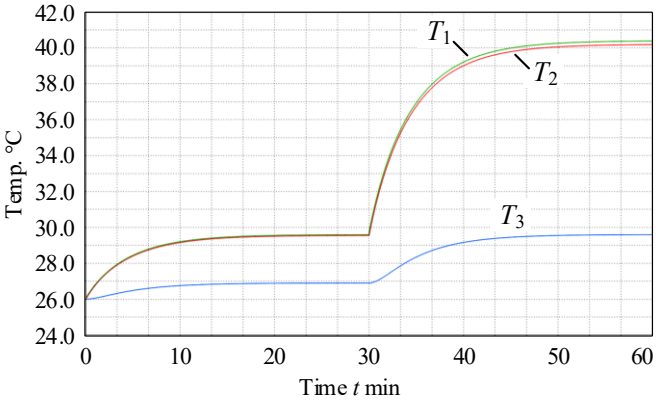

(b)

Fig. 4. Simulation result of temperature prediction and control
(a) With proposed control (b) Without control.

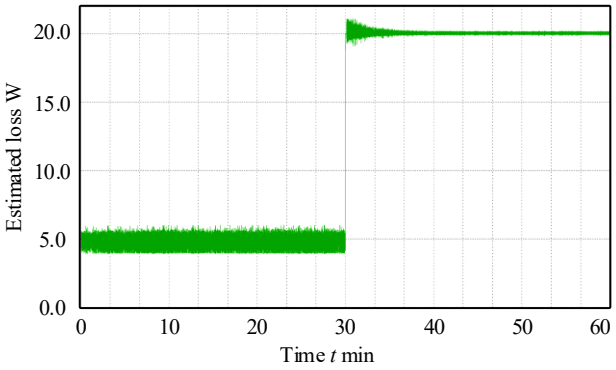

(a)

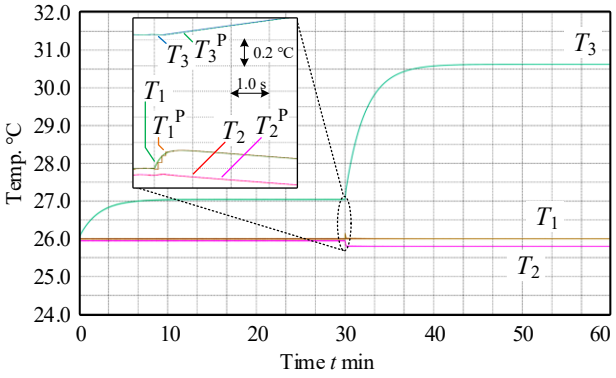

(b)

Fig. 5. Simulation result of temperature control with loss estimation
(a) Estimated loss (b) Temperature control with estimated loss.

temperature T_2 and the ambient temperature T_a as the measured value in the simulation.

Fig. 5a shows the estimated loss based on the (14). The estimated loss shows good agreement with the actual loss even if the actual loss has a step change. The maximum error rate of the estimated loss is about 22%. Fig. 5b shows the simulation result of the temperature control with the estimated loss. The predicted temperatures also closely align with the simulated values. The device temperature T_1 is controlled by the temperature command even if the loss amount has a step change.

V. Experimental Verification

Fig. 6 depicts the experimental setup of the prototype featuring the Peltier device. Each heat-spreader incorporates a Peltier device, with a resistor serving as the heater instead of the power devices on the cold side. To prevent leakage heat flow during thermal measurement, Styrofoam covers both the resistor and heat-spreader #1. It's noteworthy that the experimental parameters mirror those used in the simulation.

A. Temperature control without loss estimation

Fig. 7a presents the experimental results utilizing the prototype, while Fig. 7b illustrates the outcomes in the absence

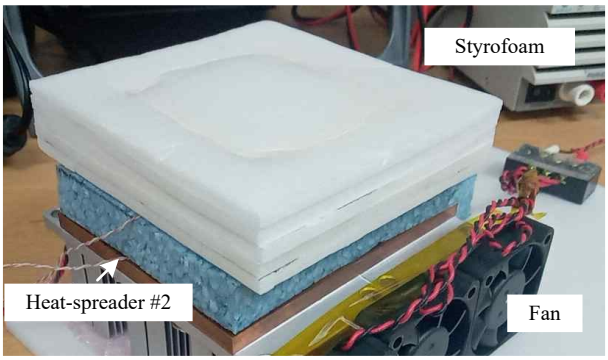

(a)

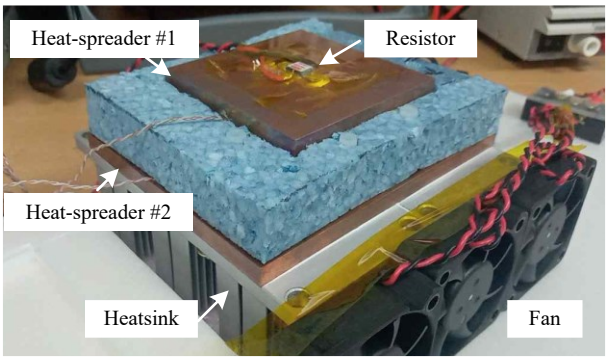

(b)

Fig. 6. Prototype. (a) With Styrofoam (b) Without Styrofoam.

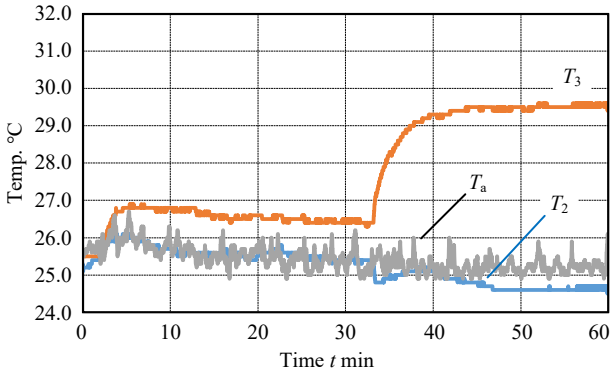

(a)

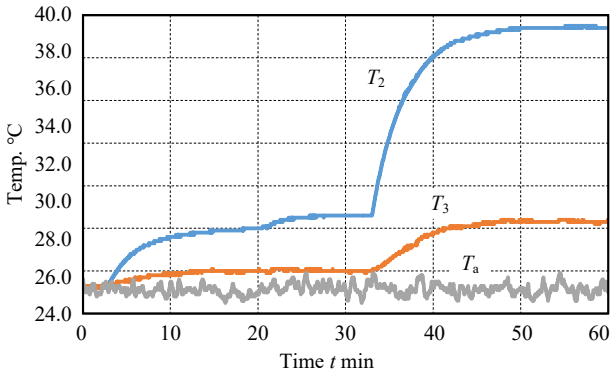

(b)

Fig. 7. Experimental result of ATC using Peltier-device (a) With control (b) Without control.

of thermal control. In the experimental setup, the loss amount and the step timing are input to the controller. Moreover, the cold side temperature T_2 remains relatively constant, except for minor fluctuations due to ambient temperature changes because the ambient temperature is not measured. The maximum temperature variance from ambient conditions is approximately 1.6 K when employing the proposed control method. Conversely, without control, this variance increases significantly to approximately 12.8 K. Consequently, the proposed control mechanism effectively reduces temperature fluctuations by 87.5%.

B. Temperature control with loss estimation

Fig. 8 presents the experimental result with the temperature control based on the estimated loss. The temperature T_2 and the ambient temperature T_a are measured by a thermocouple to estimate the loss of the resistor. The cold side temperature T_2 is also controlled to the constant. The maximum temperature difference to the command value is 0.7 K, and the maximum error rate is 2.6%.

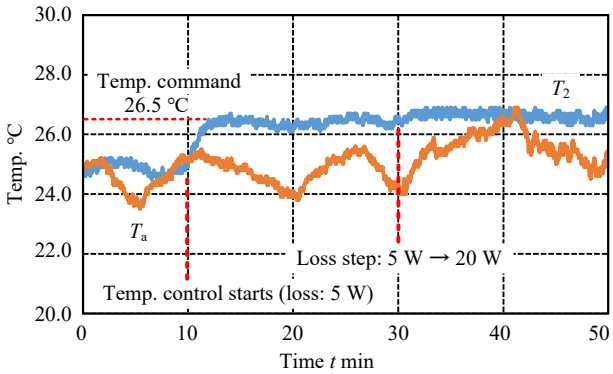

Fig. 8. Experimental result of ATC with estimated loss.

VI. Conclusion

The paper introduced an Active Thermal Control (ATC) approach utilizing a Peltier device to mitigate thermal stress on power devices. The proposed ATC did not affect the circuit operation because the additional thermal structure, which employs the Peltier device, completely controls the temperature. Model Predictive Control (MPC) was employed to regulate temperature, with the predicted temperature from a thermal model used to derive the current command for the Peltier device. Moreover, the predicted temperature and the actual temperature estimated the loss amount at the heat source without any electrical information about the heat source. Simulation results confirmed the accuracy of temperature predictions and loss estimation under MPC. Additionally, experimental validation supports the effectiveness of the proposed method, resulting in a 2.6% error rate in temperature control.

References

[1] Y. Qi, K. Ma and S. Xia, "Active Thermal Control With Optimal Phase Angle Under Stall Condition of Machine Drive Inverter," *IEEE Trans. Power Electron.*, vol. 37, no. 9, pp. 10128–10132, Sep. 2022.

[2] Y. Ko, M. Andresen, G. Buticchi, and M. Liserre, "Discontinuous-Modulation-Based Active Thermal Control of Power Electronic Modules in Wind Farms," *IEEE Trans. Power Electron.*, vol. 34, no. 1, pp. 301–310, Jan. 2019.

[3] J. Sheng et al., "Active Thermal Control for Hybrid Modular Multilevel Converter Under Overmodulation Operation," *IEEE Trans. Power Electron.*, vol. 35, no. 4, pp. 4242–4255, Apr. 2020.

[4] N. Deshmukh, A. Chanekar, S. Anand, and S. R. Sahoo, "Active Thermal Control for Buck Converter-Based Active Power Decoupling Circuit," *IEEE Trans. Power Electron.*, vol. 37, no. 12, pp. 14955–14965, Dec. 2022.

[5] J. Shen, J. Zhang, X. Huang, L. Qiu, and Y. Fang, "Active Thermal Management Method for Output-Parallel DAB DC–DC Converters Under Parameter Mismatches and Asymmetrical Modulation," *IEEE Trans. Power Electron.*, vol. 38, no. 7, pp. 8237–8248, Jul. 2023.

[6] M. P. Gupta, M. -H. Sayer, S. Mukhopadhyay, and S. Kumar, "Ultrathin Thermoelectric Devices for On-Chip Peltier Cooling," *IEEE Trans. CMPT*, vol. 1, no. 9, pp. 1395–1405, Sep. 2011.

[7] H. Morimitsu and S. Katsura, "Sensorless Control of Heat Inflow to a Thermal Display Using a Heat Inflow Observer," *IEEE Trans. Ind. Electron.*, vol. 62, no. 7, pp. 4288–4297, July 2015

[8] L. Ding, R. Song, S. Zhao, J. Wang, and H. A. Mantooth, "Active Peltier Effect Heat Sink for Power Semiconductor Device Thermal Stability Enhancement," *IEEE Trans. Power Electron.*, vol. 38, no. 9, pp. 11507–11520, Sep. 2023.